SAND2019-8713C

A Self-Guarded Hot-Plate Thermal Measurement System for Low-Thermal-Conductivity Materials

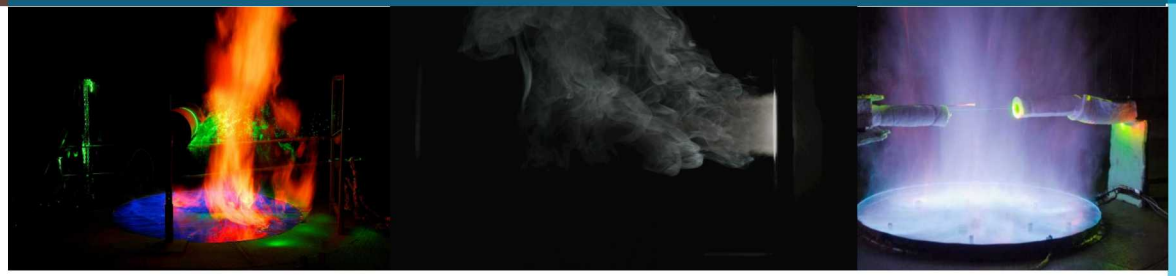

PRESENTED BY

Jeffrey D. Engerer

Sandia National Laboratories is a multimission laboratory managed and operated by National Technology & Engineering Solutions of Sandia, LLC, a wholly owned subsidiary of Honeywell International Inc., for the U.S. Department of Energy's National Nuclear Security Administration under contract DE-NA0003525.

SAND2019-####C

Outline

Thermal Measurement Systems.

Design of Hot-Plate Systems.

Sandia's Self-Guarded Hot Plate.

Proofs, Solutions, & Initial Validation Work

Future Work.

Thermal Conductivity Measurement Devices

Many methods exist for measuring thermal conductivity/diffusivity:

- Hot plate
- Transient plane/line source
- 3-Omega
- Time/Frequency-Domain Thermoreflectance
- Flash diffusivity
- etc…

For large, flat, thick samples, hot-plate measurement systems are a viable option.

Design of a Hot Plate System

Idealized Boundary Conditions

- Electric heater (known power).
- Limit transverse losses through 'guarding.'
- Standard for low temperature materials.

Steady State Analysis:

$$k = \frac{q_o'' L}{\Delta T_{ss}}$$

Physical Setup

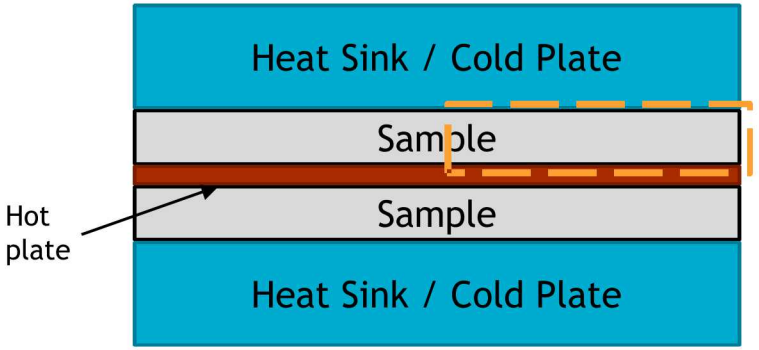

Heat Transfer BC's

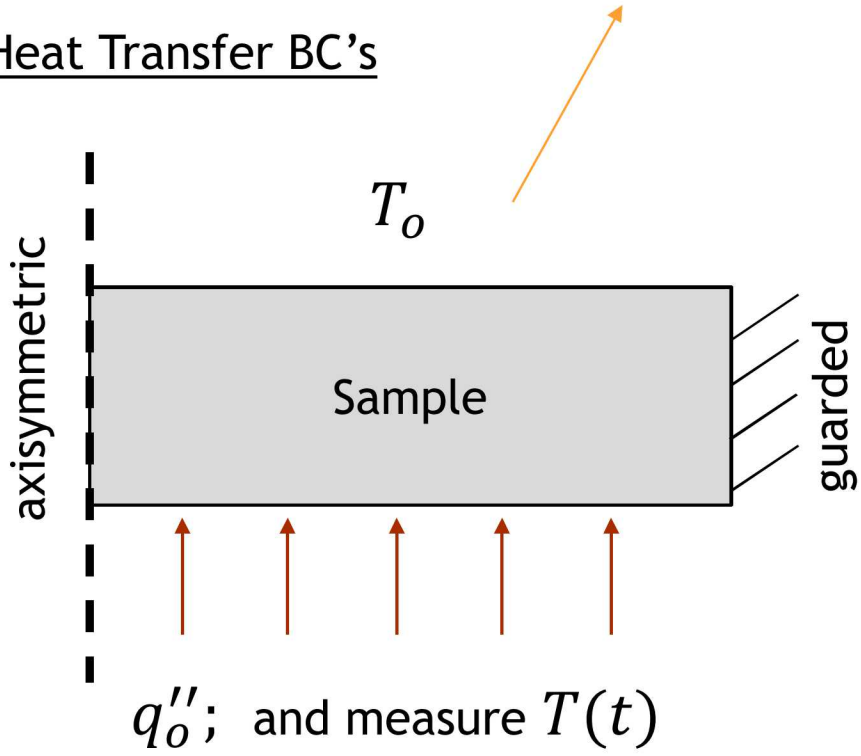

Guarded vs. Self-Guarded Hot Plates

Guarded Hot Plate

- **Conductive heater.**
  - Heat spreading / thermal averaging.
- Higher accuracy (1%).
  - J. Res. Natl. Inst. Stand. Technol. **115**, 23-59 (2010)
- More complex design/operation.

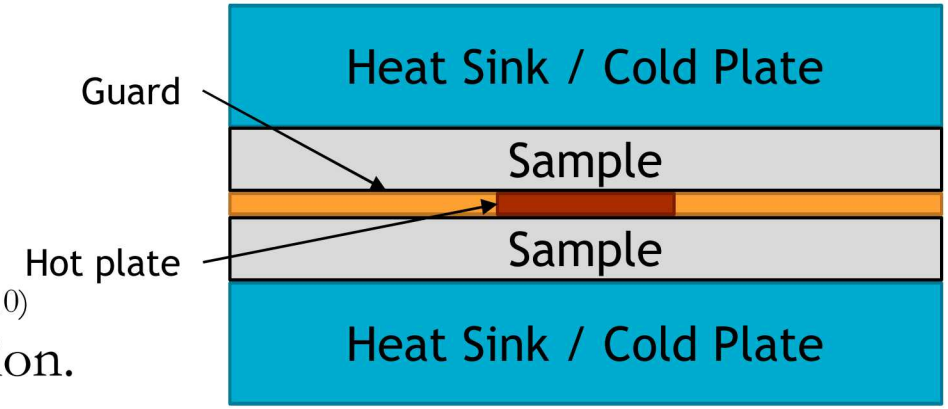

Self-Guarded Hot Plate

- Also called 'unguarded'
- **Non-conductive heater.**
  - Negligible spreading / thermal averaging.
- Lower accuracy (nearer 5-10%).
  - Could theoretically be reduced?
- Simpler design/operation.

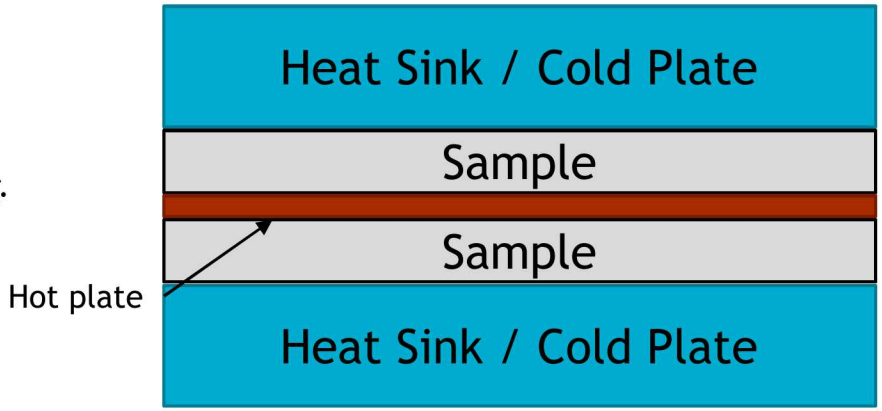

Steady-State vs. Transient Operation

Steady-State (traditional hot-plate method):

- Easy interpretation of data.
- Yields thermal conductivity (k).
- Requires very precise boundary conditions.
- Contact resistance must be accounted for (or negligible).

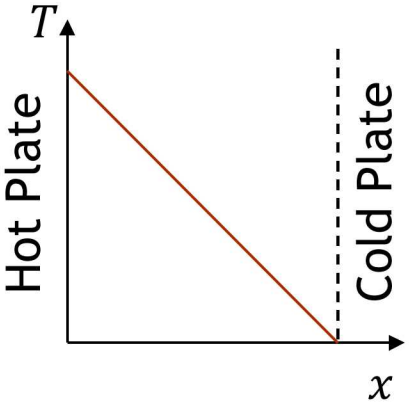

Transient (similar to transient plane source method):

- More difficult to interpret data (need analytical solution).
- Yield volumetric heat capacity (ρc_p) and conductivity (k).
- Can circumvent contact resistance and other nonidealities.
- Fewer restrictions on boundary conditions.
  - **End experiment before interactions** with non-ideal boundary conditions.
    - See: F.de Monte et al., Int. J. Heat and Mass Transf., 51 (2008) 5931–5941.

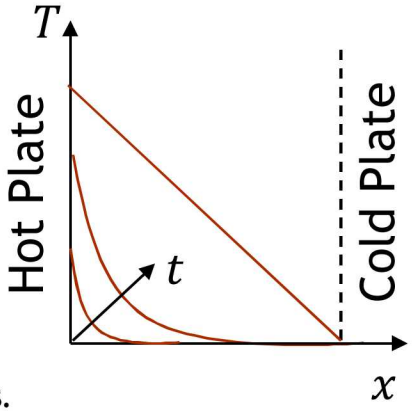

Fourier Number → $\dfrac{\alpha t_{pen}}{d^2} \approx \dfrac{0.1}{n}$

where 10^{-n} is the desired level of accuracy.

Examples: Hot Plate / Transient Plane Source

NIST 1.016-meter Hot Plate

- Guarded (w/ thermopile & heater).
- Steady State.
- Various commercial systems w/ this design.

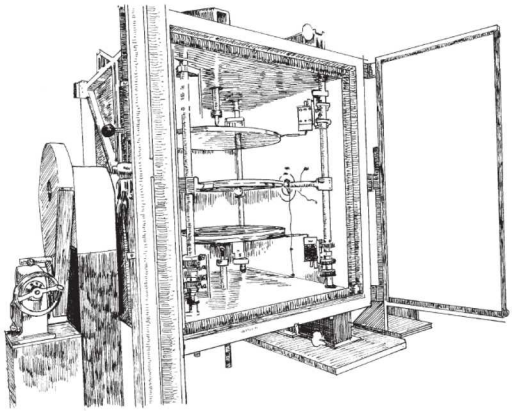

Nichrome Screen Heater

- Self-guarded.
- Steady State.

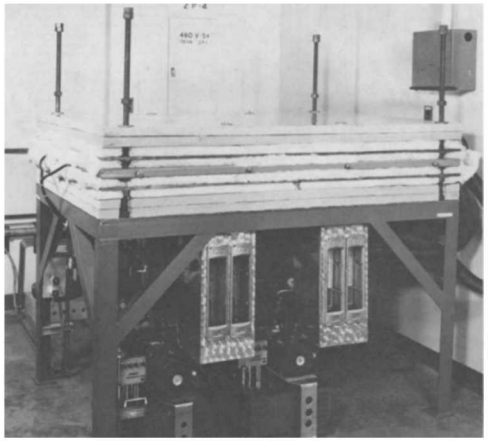

Hot Disk / Trans. Plane Source

- Self-guarded (for 1D solutions).
- Transient.

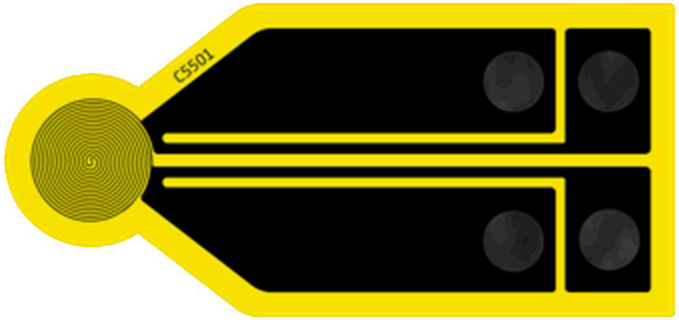

Sandia's Self-Guarded Hot Plate System

Transient operation (similar to transient plane source).

Self Guarded:

- Heater has thermal conductivity comparable-to or less-than sample.

Large aluminum heat sinks without temperature control.

- Reaches a quasi-steady state.
  - Constant gradients, as system temperature drifts upward.
- High thermal diffusivity of aluminum ensures gradients in heat sink are minimal.

Silicone rubber heater w/ TCs at interfaces.

- Discrete temperature measurements
- Most other systems use averaged heater temp.
  - Conductive heaters.
  - Platinum heater/RTD.

Original Self-Guarded System

Previous system was designed for foams (k<0.1 W/mK)

Performance limited by thermocouple placement.

- Thermocouples exacerbate contact resistance
  - For SS304 to Silicone Rubber, $R_{cont} \approx 20 \frac{cm^2 K}{W}$
    - Parihar et al. (1999) J Heat Transf. 171, 700
  - For a **1 W/mK sample**, 1 cm thick: $R_{samp} = 100 \frac{cm^2 K}{W}$

Note: Design would be acceptable for <0.1 W/mK sample

Thermocouples are in a significant thermal gradient!

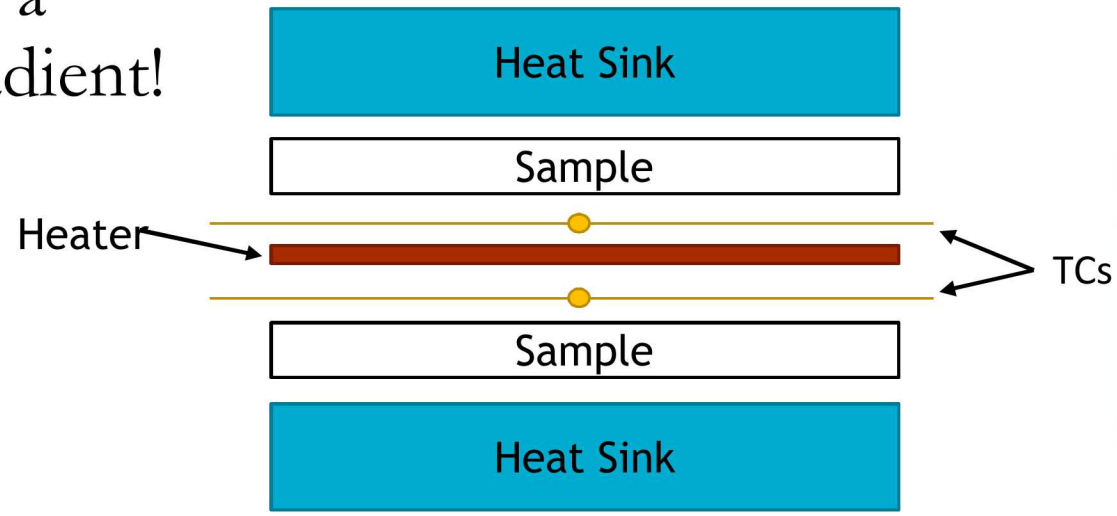

Updated Self-Guarded System

New system design allows for higher thermal conductivity samples ($k \sim 1 \frac{\mathrm{W}}{\mathrm{mK}}$)

Thermocouples no longer in thermal gradient.

Additional benefit: thermal mass of heaters substantially reduced (Kapton vs Silicone Rubber)

- Increased sensitivity to sample properties.

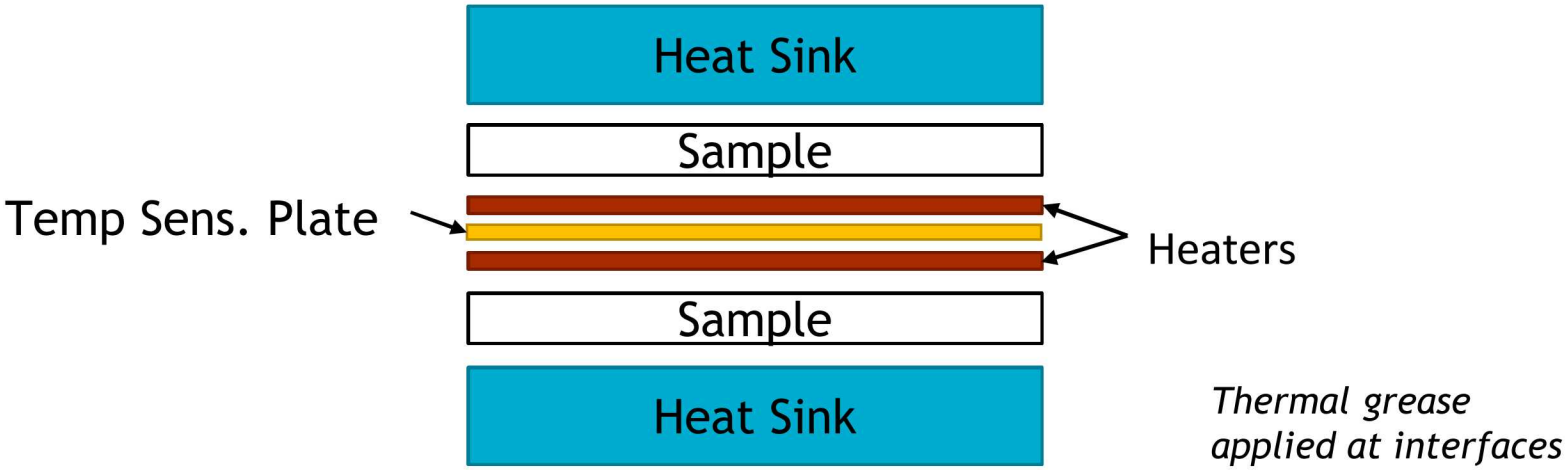

Performance of Self-Guarded Hot Plate

Demonstrate the validity of the self-guarded system by:

1. Proof for 'self-guarding.'
2. Deriving analytical solutions.
3. Perform validation experiments.
   - Reference Sample: Pyroceram 9606 (1 cm thick, 13.7 cm diameter)

Proof for the Self-Guarded Technique

Solving Green's Function:

$$T(x,r,t) - T_i = \alpha \int_{\tau=0}^{t} \int_{r'=0}^{R} \frac{q_0''}{k} G_{R01}(r,t|r',\tau) G_{X21}(x,t|0,\tau) 2\pi r' dr' d\tau$$

Sample aspect ratio of 6.85 (from our reference sample)

Errors from losses are much less than 1% at center.

Boundary Conditions:

$$T(x,r,0) = T_i$$

$$-k \left.\frac{\partial T}{\partial x}\right|_{x=0} = q_0''$$

$$T(L,r,0) = T_i$$

$$T(x,R,0) = T_i$$ Very conservative estimate for edge losses

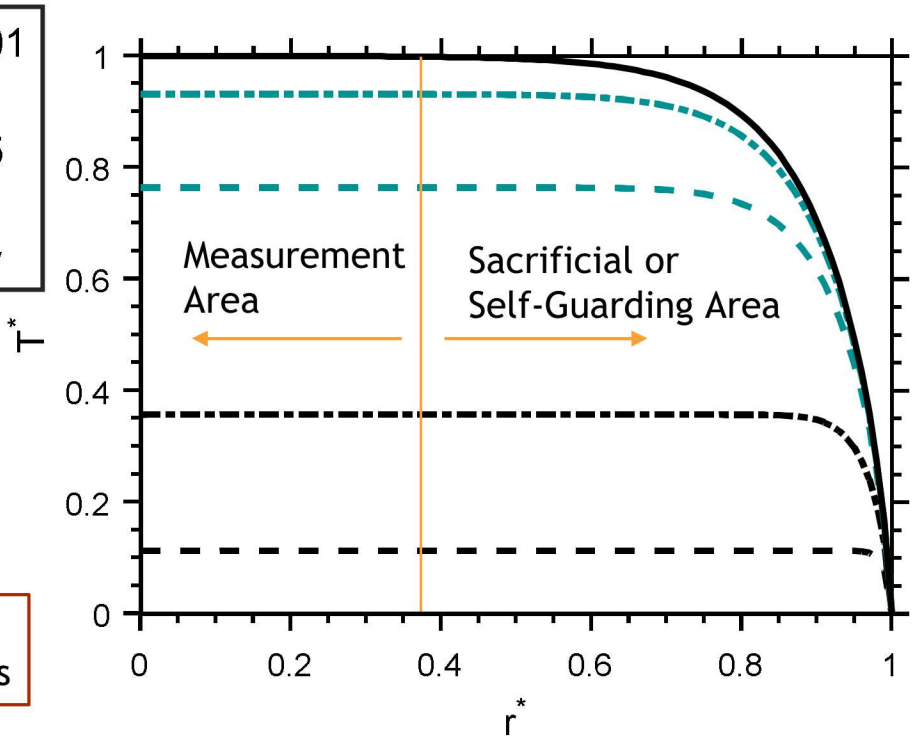

Analytical Solution

- Two-layer Heat Transfer
  - Laplace Transform, Residue Integration
  - Dynamic Heat Flux
  - Dynamic Heat Sink Temperature
  - Semi-Numerical Solution
    - Sum each timestep separately.

$$T_S(t_k) = \sum_{j=1}^{k} \Delta T_{S,j} H(t_k - t_j)$$

$$Q''_H(t_k) = \sum_{i=1}^{k} \Delta Q''_{H,i} H(t_k - t_i)$$

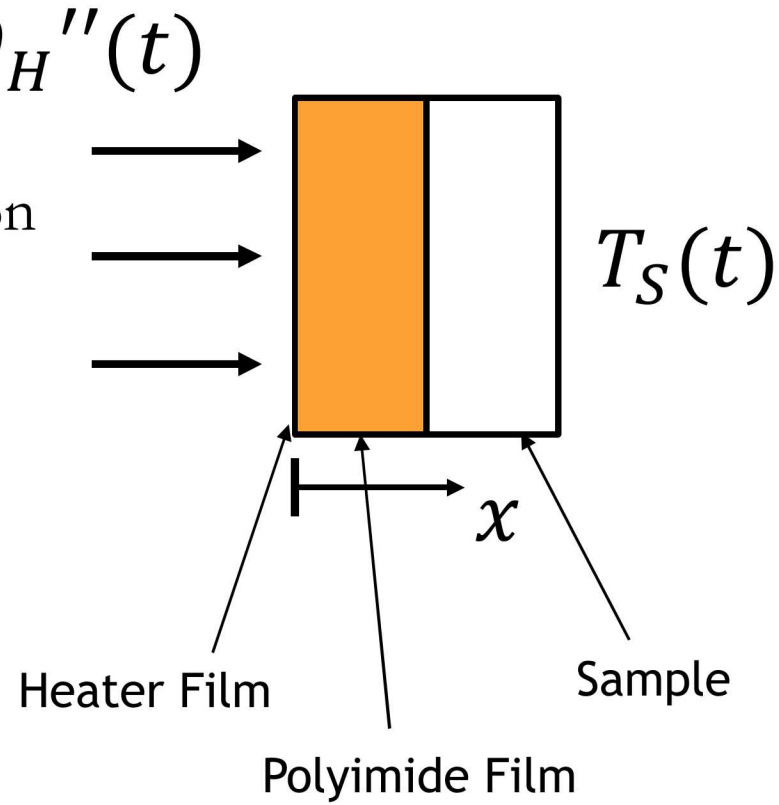

- Resulting solution has many terms/series, but very flexible.

Analytical Solution

Heater has very small time constant (~10 ms)

Theoretical results insensitive to heater beyond 50 ms.

Good temporal behavior for transient and steady state measurements.

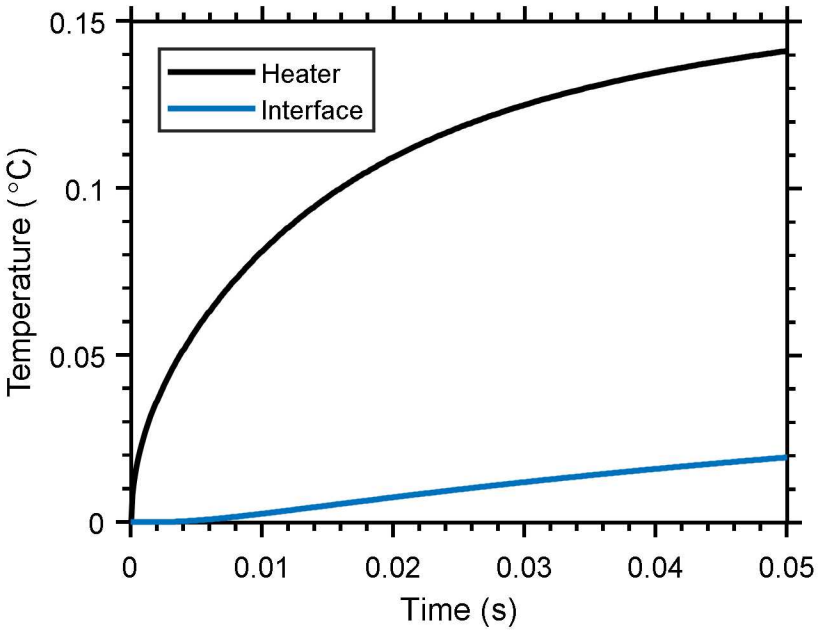

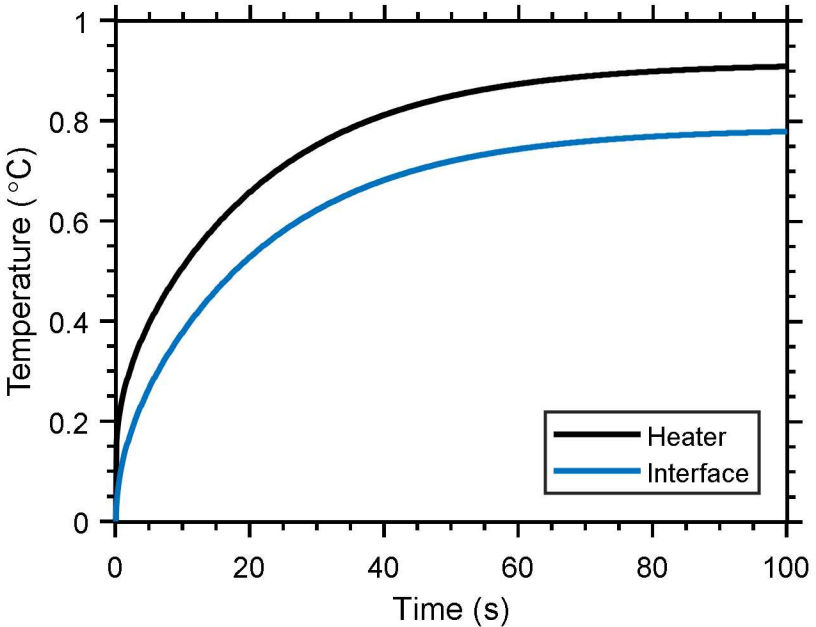

Validation Experiments

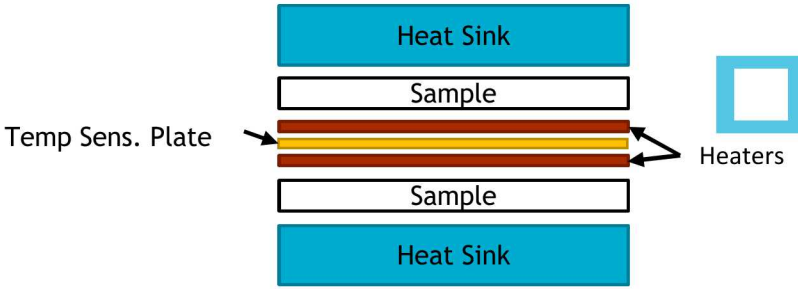

Pyroceram 9606

- Trends match analytical model.
- Scatter in heater TC temps.
  - Evidence of thermal contact issues.
- TCs may have moderate lag.

$$\frac{\text{TC heat cap.}}{\text{polyim. res.}} = \frac{\rho V c_p}{\frac{k}{L}A} \approx 0.6 \text{ s}$$

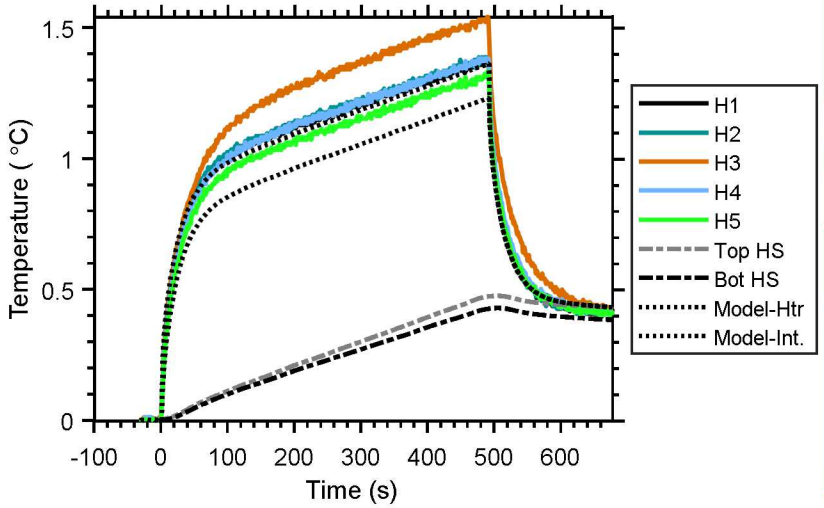

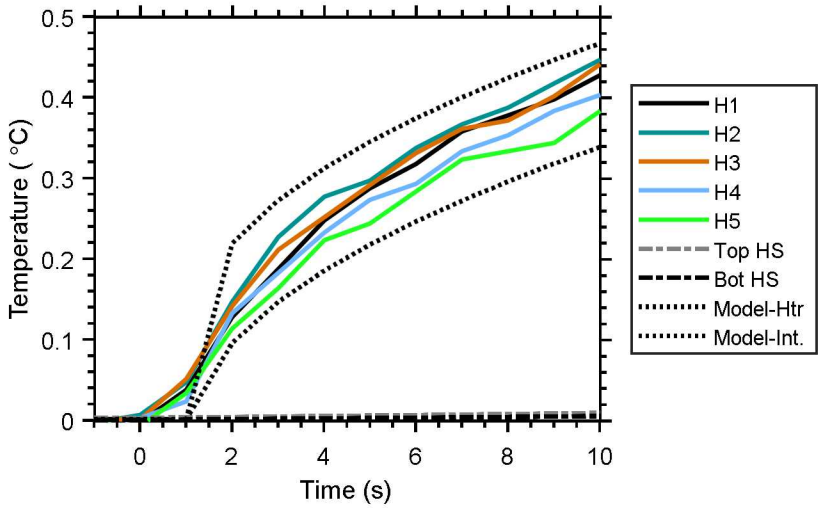

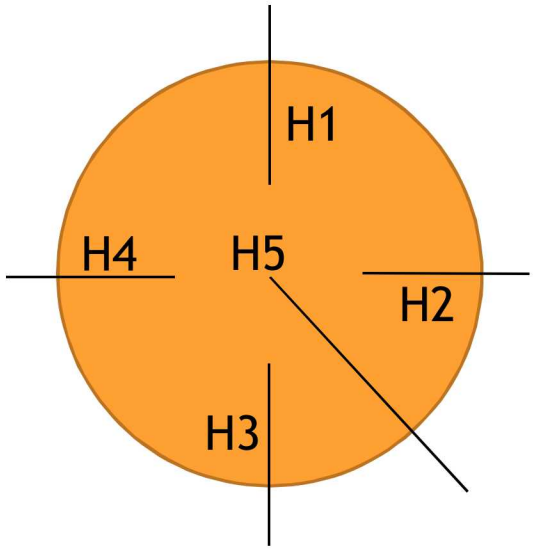

Validation Experiments

Compare TCs with H5 as reference.

- H3 has biggest issues.
- H1 and H2 have short 'time constants.'
- H3 and H4 have short and long time constants overlaid.

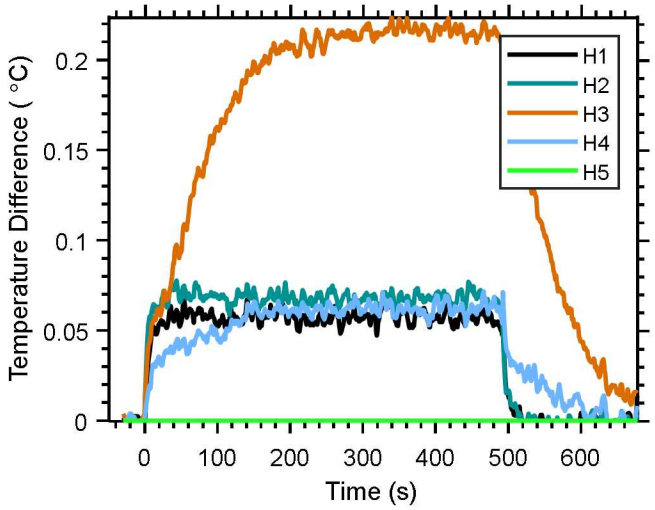

Poor, spatially varying interfacial conductance seems a likely culprit.

- Improve thermal interface (thermal grease)
- Characterize interfacial conductance.

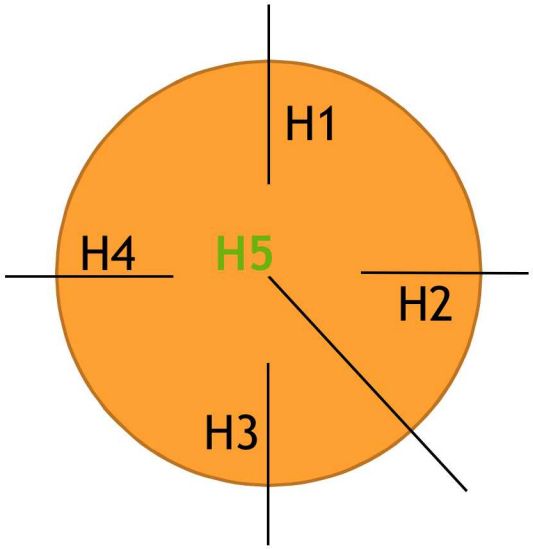

Follow-on Work

Characterize/correct performance issues.

Simple material characterization.

- For most problems, commercial systems are preferred.

Thermal properties of inhomogeneous samples.

Numerical solutions to inverse problems, complex geometries.

Conclusions

Self-guarded hot-plate is a viable design.

- Considered less accurate than guarded hot plate.
- Simpler to implement than guarded unit.
- Perhaps better for transient problems.

Implements transient plane source solutions.

- Not very effective for simple property measurements.
- Discrete temperature detection points.

Implementation at Sandia almost complete.

- Currently have some residual issues (contact resistance).

BACKUP SLIDES

Backup Slides: Self Guarding

The solution is found via the appropriate Green's functions [**?**]:

$$T(x,r,t) - T_i = \alpha \int_{\tau=0}^{t} \int_{r'=0}^{R} \frac{q_0''}{k} G_{R01}(r,t|r',\tau) G_{X21}(x,t|0,\tau) 2\pi r' dr' d\tau \tag{6}$$

which yields the solution:

$$T^*(x^*,r^*,Fo) = 4 \sum_{n=1}^{\infty} \sum_{m=1}^{\infty} \cos(\beta_n x^*) \frac{J_0(\beta_m r^*)}{\beta_m J_1(\beta_m)} \frac{1}{\beta_n^2 + \frac{L^2}{R^2}\beta_m^2} \left\{ 1 - \exp\left[-\left(\beta_n^2 + \frac{L^2}{R^2}\beta_m^2 \right) Fo \right] \right\} \tag{7}$$

where temperature is nondimensionalized as:

$$T^*(x^*,r^*,Fo) = \frac{k\left[T(x^*,r^*,Fo) - T_i\right]}{q_0'' L} \tag{8}$$

and spatial coordinates are nondimensionalized as: $x^* = x/L$ and $r^* = r/R$. The Fourier number is defined as $Fo = \alpha t/L^2$. J_0 and J_1 are Bessel functions of the first kind. The summation variables, β_n and β_m are defined as:

$$\beta_n = \pi(n - \frac{1}{2}) \tag{9}$$

and the roots of the Bessel function:

$$J_0(\beta_m) = 0 \tag{10}$$

Equation 7 was solved by summing the first 500 terms of each series; the results are provided in Figure 2 for an aspect ratio of $\lambda = 6.85$. This aspect ratio matches the reference sample, which is $1\,\mathrm{cm}$ thick and has a diameter of $13.7\,\mathrm{cm}$. The results indicate the temperature distribution at the center of the heated surface has negligible error ($1 - T^* \ll 0.01$). Measurement uncertainty on the reference sample is dominated by sources other than edge effects.

Edge effects were further characterized by performing additional runs at varying aspect ratios. Error ($1 - T^*$) exceeds 0.01 when the aspect ratio, λ, falls below four. Consequently, the recommended maximum sample thickness on this $15.24\,\mathrm{cm}$ self-guarded hot plate is $1.9\,\mathrm{cm}$, granted the overly conservative assumptions on convective losses at the perimeter. Samples moderately thicker than $1.9\,\mathrm{cm}$ can likely be accommodated, but would require better characterization of the outer boundary (e.g., demonstrating that $\mathrm{Bi} \lesssim 1$). These non-dimensionalized results are extensible to any material (regardless of thermal properties) tested in a self-guarded hot-plate system, provided the sample thermal conductivity is comparable to or greater than that of the heater assembly.

Backup Slides: Analytical Solution

$$\bar{T}_H(s) = \left[k' \sum_{j=1}^{\infty} \Delta T_j e^{-\alpha_1 t_j q_1^2} + (k_1 q_1)^{-1} \left(k' \sinh L_1 q_1 \cosh L' L_1 q_1 + \cosh L_1 q_1 \sinh L' L_1 q_1 \right) \right.$$
$$\left. \sum_{j=1}^{\infty} \Delta Q_j'' e^{-\alpha_1 t_f q_1^2} \right] / \left[\alpha q_1^2 (\cosh L_1 q_1 \cosh L' L_1 q_1 + \sinh L_1 q_1 \sinh L' L_1 q_1) \right] \quad (13)$$

where q_1 is related to the Laplace transform variable, s, as follows:

$$q_1 = \sqrt{\frac{s}{\alpha_1}} \quad (14)$$

k' and L' are ratios of the thermophysical properties:

$$k' = \frac{k_2}{k_1} \sqrt{\frac{\alpha_1}{\alpha_2}} \quad (15)$$

and

$$L' = \frac{L_2}{L_1} \sqrt{\frac{\alpha_1}{\alpha_2}} \quad (16)$$

Backup Slides: Analytical Solution

The inverse Laplace transform was performed using residue integration, by summing over the poles in Equation 13:

$$T_H = T_S(t_k) + \left(1 + \frac{L'}{k'}\right)\frac{L_1}{k_1}Q_H(t_k) - 2\sum_{n=1}^{\infty}\sum_{j=1}^{k}\frac{k'}{B}\Delta T_i H(Fo - Fo_j)e^{-y_n^2(Fo-Fo_j)} - 2\sum_{n=1}^{\infty}\sum_{i=1}^{k}\frac{A}{B}\frac{L_1\Delta Q_j''}{k_1}H(Fo - Fo_i)e^{-y_n^2(Fo-Fo_i)} \quad (17)$$

where A and B are defined as:

$$A = \frac{1}{y_n}\left(k' \sin y_n \cos L'y_n + \cos y_n \sin L'y_n\right) \quad (18)$$

and

$$B = y_n\left[(k' + L)\sin y_n \cos L'y_n + (k'L' + 1)\cos y_n \sin L'y_n\right] \quad (19)$$

and the imaginary poles, y_n, are defined by the transcendental equation:

$$k' \cos y_n \cos L'y_n - \sin y_n \sin L'y_n = 0 \quad (20)$$

The temperature at the interface also has the poles in Equation 20 and has a similar form:

$$T_H = T_S(t_k) + \frac{L_2}{k_2}Q_H(t_k) - 2\sum_{n=1}^{\infty}\sum_{j=1}^{k}\frac{k'\cos y_n}{B}\Delta T_i H(Fo - Fo_j)e^{-y_n^2(Fo-Fo_j)} - 2\sum_{n=1}^{\infty}\sum_{i=1}^{k}\frac{A\cos y_n}{B}\frac{L_1\Delta Q_j''}{k_1}H(Fo - Fo_i)e^{-y_n^2(Fo-Fo_i)} \quad (21)$$

The solution for an ideal scenario with a constant-magnitude heat flux ($0.0312\,\mathrm{W/cm^2}$) and a constant-temperature heat sink ($T_S = T_i$) using the properties in Table 1. The solution is provided in Figure 4. Thermal energy rapidly penetrates the heater, which reaches a quasi-steady internal temperature profile in much less than one second. The sample heats up more slowly, reaching steady state at roughly 100 s. The rapid thermal time constant of the heater is decoupled from the dynamic response of the sample, improving sensitivity of the measurement technique to the thermal properties of the sample. These results confirm the simplified calculations presented previously in Section 2.1.